PROCEEDINGS OF SCIENCE

The optical module of the Baikal-GVD neutrino telescope

A.D. Avrorin[a], A.V. Avrorin[a], V.M. Aynutdinov[a], R. Bannash[g], I.A. Belolaptikov[b], D.Yu. Bogorodsky[c], V.B. Brudanin[b], N.M. Budnev[c], I.A. Danilchenko[a], G.V.Domogatsky[a], A.A. Doroshenko[a], A.N. Dyachok[c], Zh.-A.M. Dzhilkibaev[a], S.V. Fialkovsky[5], A.R. Gafarov[c], O.N. Gaponenko[a], K.V. Golubkov[a], T.I. Gress[c], Z. Honz[b], K.G. Kebkal[g], O.G. Kebkal[g], K.V. Konischev[b], A.V. Korobchenko[b], A.P. Koshechkin[a], F.K. Koshel[a], A.V. Kozhin[d], V.F. Kulepov[e], D.A. Kuleshov[a], V.I. Ljashuk[a], M.B. Milenin[e], R.A. Mirgazov[c], E.R. Osipova[d], A.I. Panfilov[a], L.V. Pan'kov[c], E.N. Pliskovsky[b], M.I. Rozanov[f], E.V. Rjabov[c], B.A. Shaybonov[b], A.A. Sheifler[a], M.D. Shelepov[a], A.V. Skurihin[d], A.A. Smagina[b], O.V. Suvorova[a], V.A. Tabolenko[c], B.A. Tarashansky[c], S.A. Yakovlev[g], A.V. Zagorodnikov[c], V.A. Zhukov[a], and V.L. Zurbanov[c]

[a] *Institute for Nuclear Research, 60th October Anniversary pr. 7A, Moscow 117312, Russia*
[b] *Joint Institute for Nuclear Research, Dubna 141980, Russia*
[c] *Irkutsk State University, Irkutsk 664003, Russia*
[d] *Skobeltsyn Institute of Nuclear Physics MSU, Moscow 119991, Russia*
[e] *Nizhni Novgorod State Technical University, Nizhni Novgorod 603950, Russia*
[f] *St. Petersburg State Marine University, St. Petersburg 190008, Russia*
[g] EvoLogics GmbH, Berlin, Germany

The Baikal-GVD neutrino telescope in Lake Baikal is intended for studying astrophysical neutrino fluxes by recording the Cherenkov radiation of the secondary muons and showers generated in neutrino interactions. The first stage of Baikal-GVD will be equipped with about 2300 optical modules. Each of these optical modules consists of a large area photomultiplier R7081-100 made by Hamamatsu Photonics and its associated electronics housed in a pressure resistant glass sphere. We describe the design of the optical module, the front-end electronics and the laboratory characterization and calibration before deployment.

The 34th International Cosmic Ray Conference
30 July- 6 August, 2015
The Hague, The Netherlands

PoS(ICRC2015)1163

1. Introduction

The objective of the Baikal Project is the creation of a kilometer-scale high-energy neutrino observatory: the Gigaton Volume Detector (GVD) in Lake Baikal [1 - 6]. The first phase of GVD will consist of 12 clusters of strings - functionally independent subarrays connected to the shore by individual electro-optical cables. In April 2015 the first cluster of Baikal-GVD was deployed in Lake Baikal and put into operation. This sub-detector was named DUBNA. It encloses 1.7 Megatons of the fresh waters of Lake Baikal. The first cluster of Baikal-GVD comprises a total of 192 optical modules (OM) arranged at eight 345 m long strings, as well as an acoustic positioning system. Seven side strings are located at 40 m distances from a central one. Each string comprises 24 OMs spaced by 15 m at depths of 900 m to 1250 m below the surface. An optical module contains a large area photomultiplier R7081-100 that detect Cherenkov radiation produced by relativistic charged particles passing through the water. The information from the ensemble of OMs allows reconstruction of direction and energy of the parent neutrino. Optical modules are the key elements of neutrino telescope. The present paper presents the design and performance of the components of the optical module, and describes selected results of the tests of 87 OMs that were prepared for the installation to the first Baikal-GVD cluster.

2. Architecture of the Baikal-GVD data acquisition system

The architecture of the data acquisition system (DAQ) of the Baikal-GVD neutrino telescope [7] determines the design and functionality of the optical module. The basic elements of the DAQ is a *section*, that comprises 12 OMs and a Central electronics Module (CeM). The block diagram of a section is presented in Fig. 1.

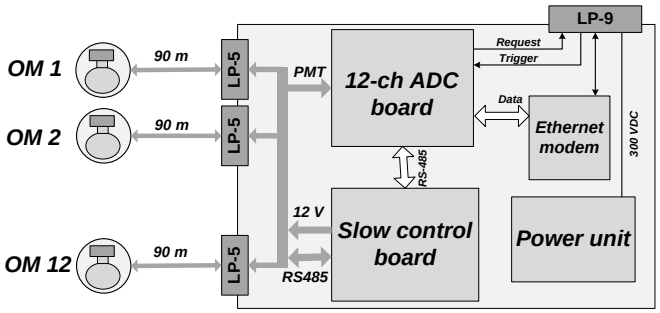

Figure 1. Block diagram of a GVD section.

PMT signals from 12 OMs are transmitted to the CeM via 90 meters of coaxial cables, where they are digitized by custom-made 12-channel ADC boards with 200 MHz sampling rate. The slow-control board located in the CeM provides data communication between OM and CeM via an underwater RS-485 bus. Also, this unit is intended for OM power control (to switch power on/off for each optical module independently). The ADC board provides trigger logic, data readout and digital processing, and connection via local Ethernet to the cluster DAQ center. According to the scheme of the *section* operation, the basic functions of the OMs are the detection of the particle radiation, the shaping of the output analog pulse for signal transmission to the ADC board, the control of the PMT operation modes, and the calibration and monitoring of

the parameters of OM electronic components. The procedures of OM calibration are described in [8].

3. The Optical Module design

A sketch of a GVD optical module is presented in Fig. 2. The OM contains a photomultiplier tube (PMT) enclosed in a transparent, nearly spherical pressure housing (VITROVEX) with 42 cm diameter. The optical contact between the photocathode region of the tube and the pressure sphere is provided by optically transparent silicon gel. A high permittivity alloy cage surrounds the PMT, shielding it against the Earth's magnetic field. A vacuum valve allows evacuating the sphere down to 0.7 atm. The OM is equipped by one deep-underwater connector (SubConn Low Profile 5-contacts). It is used for analog pulse transmission, slow control (2-wire RS-485) and OM power supply (12 VDC). The OM electronics unit is mounted directly on the PMT base.

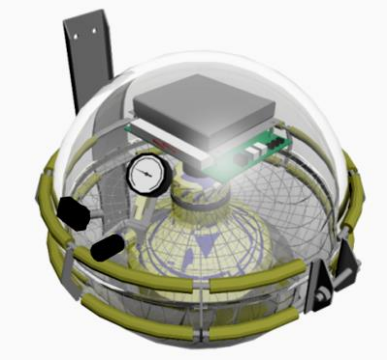

Figure 2. The Baikal-GVD optical module.

After testing different options for the photomultiplier, Hamamatsu R7081-100 was selected as a light sensor for the OM. This PMT has a hemispherical SBA photocathode with 10" diameter and quantum efficiency up to 35%. The basic PMT parameters are presented in the Table 1.

Table 1. Hamamatsu specifications for10" R7081-100 photomultiplier tubes

Spectral response	300 to 650 nm
Quantum efficiency at peak	35%
Max. supply voltage for gain 10^7	2000 V
Dark count at 25 deg. C	8000 Hz
Transit time spread (FWHM)	3.4 ns
Peak to valley ratio	2.8
Pulse linearity at 2% deviation	40 mA

The block diagram of the optical module electronics is presented in Fig. 3. The OM electronics includes a controller, a high voltage (HV) power supply unit, a fast two-channel amplifier, and a LED flasher. The OM controller is intended for communication to CeM, for HV regulation and monitoring, for PMT noise measurements, and for time and amplitude calibration with LEDs. It is designed by SNIIP-AUNIS Ltd (Russia) on the basis of the SiLabs C8051F121 microcontroller.

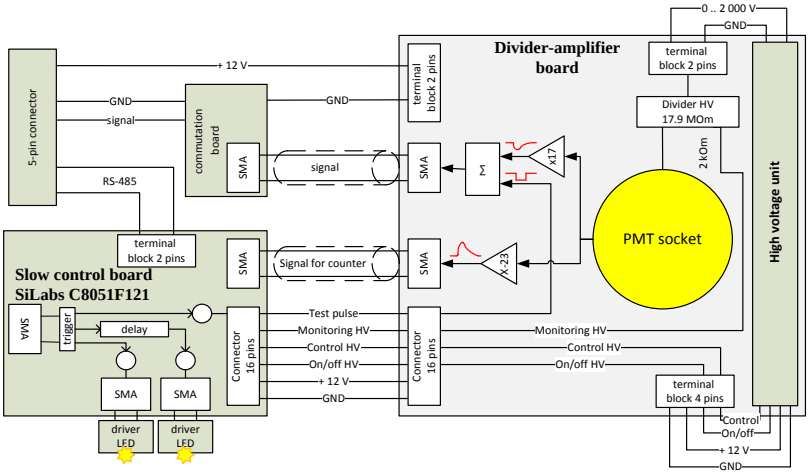

Figure 3. Block diagram of the OM electronics.

Slow control data to and from the OMs are transferred via an underwater RS-485 bus. The unit has an instruction set for the control of OM electronics: HV control (to switch HV on/off, to set PMT voltage and readout HV value), LED flasher control (to set LED intensities, the delay between LED pulses, and the period of flashes), the counter control (setting counter threshold, time window, off-duty factor and the size of circular memory data buffer). Also a set of procedures is foreseen for the laboratory calibration of the counter threshold and PMT voltage.

The PMT power supply is provided by a passive HV divider circuit with the resistance of 18 MΩ and HV unit (SHV 12-2.0 K 1000 P produced by TRACO Electronic AG) with positive polarity. The tube gains have been adjusted to about 10^7.

The PMT amplifier is comprised of two channels. The first channel with an amplification factor of 14 forms a signal with negative polarity that is transmitted to the ADC board. The second channel with an amplification factor of 21 produces positive pulses that are intended for PMT noise monitoring. The outer cascades are implemented as emitter-follower amplifiers and provide operation with 50Ω load. The maximum amplitude for both channels is limited to 4 Volts.

The LED flasher is intended for time and amplitude calibration of OM channels during long-term exposition. It includes two LEDs Kingbright L7113 with a dominant wavelength about 470 nm. The LED pulse has a width of ~6 ns (FWHM). The control system of the flasher has to provide independent tuning of two LED luminosities in a wide dynamic range (up to about 10^8 photons per LED flash) and has to have a minimal level of cross-talk between two LED channels (less than 1%).

The OM counter with programmable threshold is intended for PMT count rate monitoring. Count rate data is accumulated in the circular buffer and transmitted to the shore for each OM.

4. OMs calibration and characterization

Before OM deployment in Lake Baikal a series of a test procedures is foreseen. There are tests of all OM electronic components, stress tests, and check up of the OM in various modes of operation (final OM tests before transportation to Baikal). Final OM tests are performed by means of a digital storage oscilloscope (LeCroy HDO 4034, 350MHz bandwidth, 0.4 ns samples, 4 channels). Four OMs are housed in a screened dark box and are connected to the oscillo-

scope inputs with 90 m coaxial cables, identical to the underwater OM cables. The test procedures are performed after at least 2 hours exposition in the darkness with PMT high voltage switched on. Internal LEDs of the OMs are used as calibration light sources. The OM test procedures are fully automatized and comprise a set of measurements of the time and amplitude parameters of the OMs.

The first stage of the OM test procedure is an adjustment of the PMT power supply voltages to provide OM channel gains about 10^8. An OM analog channel comprises PMT, preamplifier and 90 m coaxial cable connecting OM and CeM. Taking into account signal amplification with the preamplifier (k_{amp}=14) and pulse attenuation in the cable (k_{att} = 0.7), a 10^8 channel gain corresponds to a PMT gain about 10^7.

The OM channel gains were derived on the basis of the single photoelectron distributions (SPE spectrums) of the PMTs obtained with LED sources. Intensities of the LEDs were adjusted to provide a detection probability of SPE signals of 10%. The SPE pulse detection thresholds were about 0.2 SPE pulse amplitude. The oscilloscope input was triggered by the synchronization signal of the LED pulse generator. The check for pedestal and noise contributions was done with the LED light output disabled. A typical pedestal-subtracted SPE charge histogram and the distribution of the OMs on SPE charge resolution are presented in Fig. 4. The SPE charge resolution is defined as one standard deviation of the SPE spectrum. The contribution of multi-electron pulses in the SPE spectrum overestimates the SPE charge resolution by about 20%.

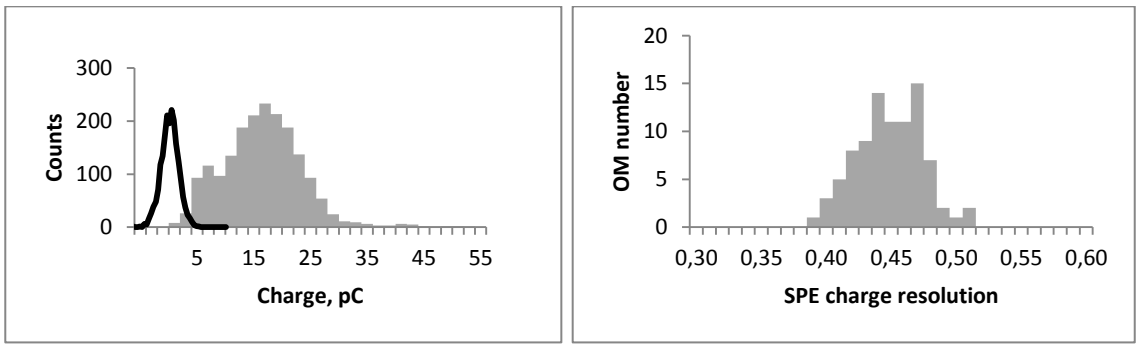

Figure 4. Typical pedestal-subtracted SPE charge distribution at PMT gain ~1×10^7 and pedestal peak (left), and distribution of the OMs on SPE charge resolution (right).

The results of the high voltage adjustment are presented in the Fig. 5. The channel gain 10^8 is provided by divider voltages between 1150 V and 1750 V for the investigated set of PMTs. Adjusted channel gains are about 1×10^8.

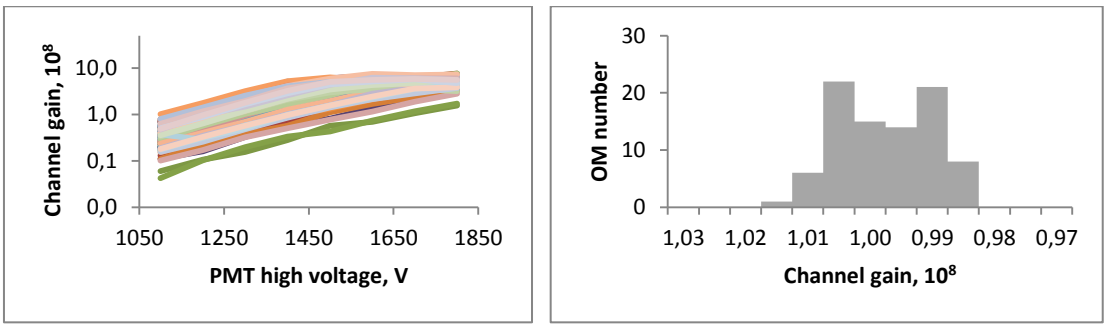

Figure 5. Dependences of the channel gains on high voltage for the set of 87 OMs (left), and OMs distribution on the fitted channel gain (right).

The OM time resolution is defined as the standard deviations of hit times of the SPE pulses. Hit times are defined as the points where each waveform of SPE pulse reached 50% of its maximum. The distribution of the OMs on the time resolution is presented in Fig. 6.

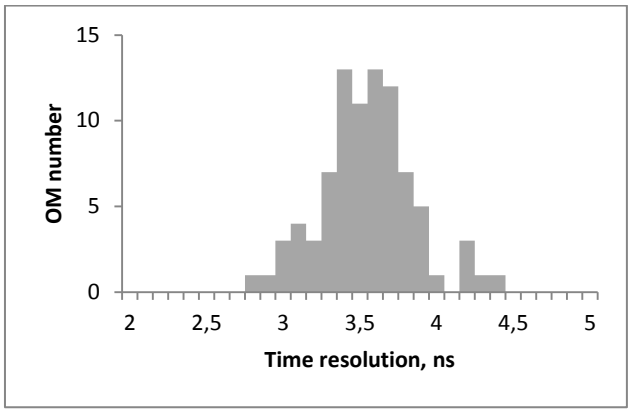

Figure 6. Distribution of the OMs on the time resolution.

There are two sources of the measuring channel nonlinearity: the limitation of the allowed PMT amplitude values by preamplifier and PMT signal saturation. To study the nonlinearity of measuring channels, the PMTs were illuminated with LED pulses of various brightness A variable $S=Q/(N_{pe}\times Q_{pe})$ has been used for evaluation of the PMT saturation behavior. Here Q is the measured charge, Q_{pe} – the charge of an SPE signal, N_{pe} – the number of photoelectrons in the pulse. The PMT amplitudes in terms of the photoelectrons in the range of the channel nonlinearity were estimated using the method of the summation of the light pulses produced by two LEDs. The dependences of S on the number of photoelectron (nonlinearity curves) are presented in Fig. 7 for 87 OMs. The linearity range of a channel is about 10^2 p.e. The solid line in Fig. 7 is a common approximation of nonlinearity curves of all tested OMs by the function $y = 1 / (1+D)$, were $D = (\lg N_{pe} / x_0)^P$, $x_0 = 2.68$, $p = 8.67$. The analytical approximations of the nonlinearity curves of the individual measuring channels allow estimating the number of recorded photoelectrons N_{pe} with 10% precision up to about 10^3 p.e.

The effect of the channel saturation influences the precision of the measured hit times of the pulses. The hit time is selected as the point where the waveform of the pulse reaches 50% of its maximum. The typical dependence of the hit point shift Δt on the number of photoelectrons in the pulse is presented in Fig. 8. In the range up to about 50 p.e. Δt is less than 1 ns.

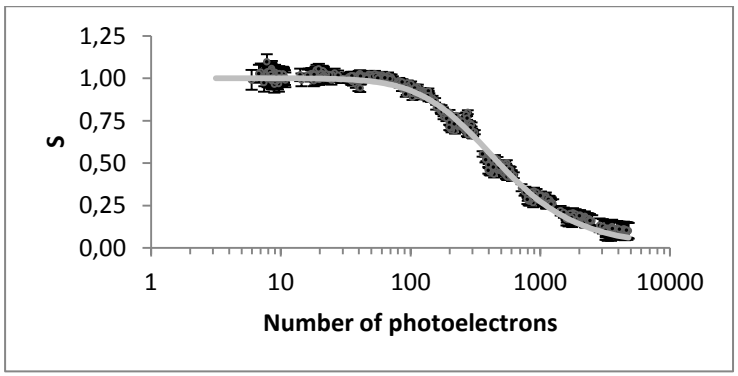

Figure 7. The nonlinearity curve of the measuring channels.

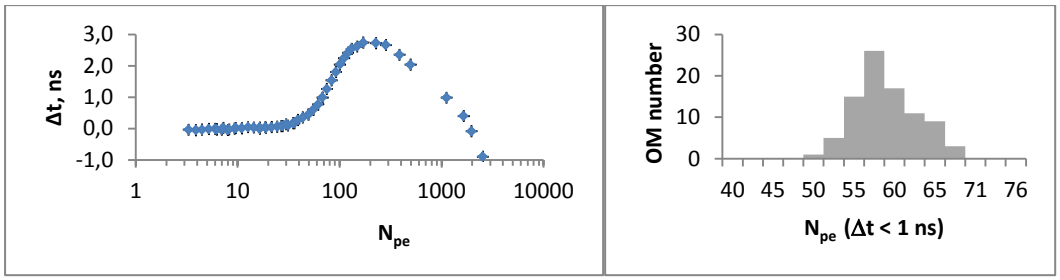

Figure 8. Dependence of the hit point shift Δt on the number of photoelectrons in the pulse N_{pe} (left), and distribution of the OMs w.r.t. N_{pe} range corresponding to Δt less than 1 ns (right).

Afterpulses are a common feature of PMTs, and are attributed to ionization of residual gases by electrons accelerated in the space between dynodes. Afterpulse measurements were made with LED pulses of about 5 ns width. The total charge of the afterpulses ($N_{pe\ afterpulses}$) was measured in the range from 300 ns up to 50 μs after the main pulse, in steps of 500 ns and for various LED intensities. $N_{pe\ afterpulses}$ grows almost linearly with the flash brightness. We characterize the OM afterpulses by the parameter $R = N_{pe\ afterpulses} / N_{pe\ main\ pulse} \times 100\%$. The typical dependence of R on the time after the main pulse is presented in Fig. 9.

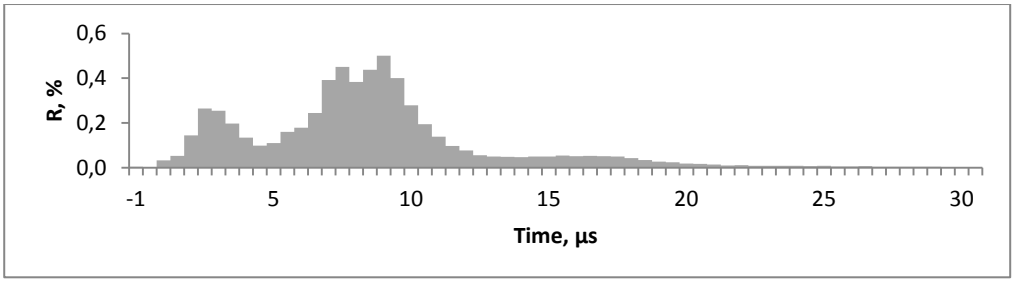

Figure 9. The typical time dependence of the afterpulse charges for primary pulses with one photoelectron.

The distribution of the OMs on the integral charge from 0.3 μs to 30 μs is presented in Fig. 10. For most of the OMs, the integral charges of the afterpulses correspond to about 0.10 … 0.15 SPE per primary photoelectron.

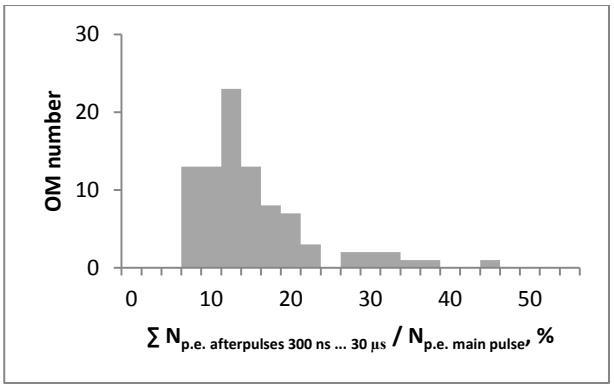

Figure 10. The distribution of the OMs on the integral charge of the afterpulses.

A total of 80 optical modules from the set of tested OMs were installed in Lake Baikal in April 2015 and form the first Baikal-GVD cluster. All OMs components are successfully operating now.

5. Conclusion

Optical modules are the key elements of the Baikal-GVD. For the OM mass production a fully automatized test facility was designed. The test of the OM performance with this facility provides information about the basic OM parameters: SPE spectrum, time resolution, systematic shifts of the hit time in dependence on the pulse amplitude, saturation curve, and afterpulses probability. These data are used as input for the detailed simulation of the Baikal-GVD physics events.

This work was supported by the Russian Found for Basic Research (grants 13-02-12221, 14-02-00175, 14-02-00972).

References

[1] A. Avrorin et al., *The prototyping/early construction phase of the BAIKAL-GVD project, NIM* **A742** 82.
[2] V. Aynutdinov et al., *The prototype string for the km3-scale Baikal neutrino telescope, NIM* **A602** 227.
[3] V. Aynutdinov et al., *The BAIKAL neutrino experiment, NIM* **A626** 13**.**
[4] V. Aynutdinov et al., *The gigaton volume detector in Lake Baikal, NIM* **A639** 30**.**
[5] A. Avrorin et al., *Current status of the Baikal-GVD project, NIM* **A725** 23**.**
[6] A. Avrorin et al., *Status and recent results of the Baikal-GVD project, Phys. of Part. and Nucl.* **46** 211**.**
[7] A. Avrorin et al., *Data acquisitions system of the NT1000 Baikal neutrino telescope, Instr. and Exp. Tech.* **57** 262**.**
[8] A. Avrorin et al., *Time and amplitude calibration of the Baikal-GVD neutrino telescope,* this Proceedings**.**
[9] A. Avrorin et al., *The first construction phase of the Baikal-GVD neutrino telescope,* this Proceedings**.**